Virtual Whiskers: Spatial Directional Guidance using Cheek Haptic Stimulation in a Virtual Environment

Fumihiko Nakamura
f.nakamura@imlab.ics.keio.ac.jp
Keio University
Yokohama, Kanagawa, Japan

Adrien Verhulst
adrienverhulst@star.rcast.u-tokyo.ac.jp
The University of Tokyo
Meguro-ku, Tokyo, Japan

Kuniharu Sakurada
kh.sakurada@imlab.ics.keio.ac.jp
Keio University
Yokohama, Kanagawa, Japan

Maki Sugimoto
sugimoto@imlab.ics.keio.ac.jp
Keio University
Yokohama, Kanagawa, Japan

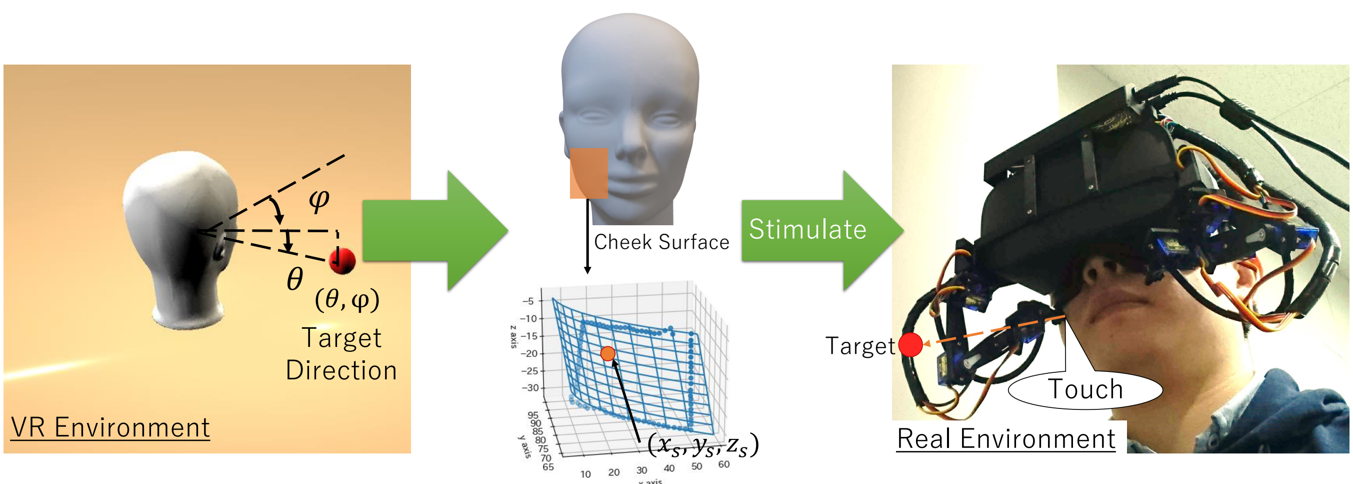

Figure 1: Spatial directional guidance with cheek haptic stimulation. Left: The target (red sphere) is located in a virtual space. The direction of the target is represented by the azimuthal angle φ and the elevation angle θ in spherical coordinate. Center: The azimuthal and angle (θ, φ) are mapped to a point on a cheek surface (x_s, y_s, z_s). The spatial direction in the virtual space is mapped to a cheek position in real space. Right: The robot arm moves to the point on the cheek and touches to cheek surface. Thus our system presents the direction of the target in virtual space to a user.

ABSTRACT

Spatial cues are an important element of navigating people in physical/virtual spaces. In terms of spatial navigation, integrating vision with other modalities, such as haptics, can guide users more effectively. Haptic cues are presented on the body parts that are sensitive to stimuli such as hands and a head. The head is reported to be superior to the body for spatial directional perception. In this paper, we propose Virtual Whiskers, a spatial directional guidance technique by haptic stimulation of the cheeks using tiny robot arms attached to a Head-Mounted Display (HMD). We deploy photo reflective sensors attached to the tip of 2 robotic arms to detect the distance between the tip and the cheek surface. Using the robot arms, we stimulate a point on the cheek obtained by calculating an intersection between the cheek surface and the target direction. We experimentally investigated how accurately participants identify the target direction provided by our guidance method. We evaluated an error between the actual target direction and the participant's pointed direction. The experimental result shows that our method achieves the average absolute directional error of 2.76 degrees in the azimuthal plane and 7.32 degrees in the elevation plane. We also conducted a spatial guidance experiment to evaluate task performance in a target search task. We compared the condition of only vision and vision with haptics for task completion time. The average of task completion time in visual-only condition was M=12.45 s, SD=14.51 s, and visual with haptic condition resulted in M=6.91 s, SD=5.48 s. Statistical test revealed a significant difference in task

AHs '21, February 22–24, 2021, Rovaniemi, Finland

ACM ISBN 978-1-4503-8428-5/21/02...$15.00
https://doi.org/10.1145/3458709.3458987

completion time between the visual condition and the visual+haptic condition.

CCS CONCEPTS

• **Human-centered computing** → **Haptic devices**; **Virtual reality**.

KEYWORDS

spatial guidance, facial haptics, virtual reality, robot arm

ACM Reference Format:

Fumihiko Nakamura, Adrien Verhulst, Kuniharu Sakurada, and Maki Sugimoto. 2021. Virtual Whiskers: Spatial Directional Guidance using Cheek Haptic Stimulation in a Virtual Environment. In *Augmented Humans International Conference 2021 (AHs '21), February 22–24, 2021, Rovaniemi, Finland.* ACM, New York, NY, USA, 11 pages. https://doi.org/10.1145/3458709.3458987

1 INTRODUCTION

In this paper, we present Virtual Whiskers, a spatial directional guidance system attached to a Head-Mounted Display (HMD) with facial haptic stimuli to cheeks.

Spatial guidance cues are essentials in Virtual Reality (VR) applications. Most of them rely solely on visual perception, but VR already has a lot of visual information to process (arguably, more than in real-life), and too much visual information can cause visual overload [23]. Some rely instead on audio-visual perception to reduce the visual workload, but they also have an effect on the workload since both the visual/audio coordinates need to be transformed to the body coordinate [16] and the head/eyes typically need to look at the visual/audio target. Another approach is to use haptic cues [28], which are less likely to be overloaded, are already mapped to the body coordinate, and do not require to look at the target.

Previous works already used haptic-based guidance successfully [4, 9], mostly by relying on vibrotactile stimulation. A vibrotactile system is easy to use but needs to be placed over the targeted zone and provide limited information.

Moreover, in a haptic-based guidance task, where precision matters, not only the type of stimulation (vibration, pressure, wind, etc.), but also the positioning of the stimuli need to be considered. Indeed, if the head is stationary, the position of haptic stimuli tends to be perceived relatively to a body-centered reference frame [27] (i.e., the body midline); else if the head is not stationary (like in a VR application), the stimuli tend to be perceived relatively to an eye-centered reference [20]. If the haptic stimuli are on the torso when the head moves, there is a shift of the perceived position of the stimulation [10].

With facial haptic stimuli at the eye-level, we can avoid having two reference frames when the head is non-stationary. A previous study on facial haptics revealed that checks' facial haptic was better in localization perception compared to the forehead and to above the eye-brow [8]. Several facial-based systems have been developed, such as winds [29] and ultrasounds [8].

With the advent of consumer VR Head Mounted Display (HMD), consumer VR Haptic devices have been released to the market [1] [2].

[1]bhaptics, https://www.bhaptics.com/tactsuit/

[2]HaptX | Haptic gloves for VR training, simulation, and design, https://haptx.com/

Those devices typically stimulate hands (e.g., haptic gloves), waist (e.g., haptic belt), or the body (arms, legs, chest, etc.; e.g., haptic suit). Nevertheless, there are not many devices targeting the user's face, despite the excellent sensitivity of the facial region [22].

In this study, we propose an HMD-based facial haptic system that provides stimulus to the cheeks. It consists of Two robotic arms attached to the bottom side of an HMD (c.f., Fig. 4) with proximity sensors. We investigate how haptic cues on the cheek provide directional information; and how facial haptic cues allow spatial guidance in a Virtual Environment (VE). Our contributions are as follow:

- Cheek stimulation by robot arms integrated with HMD to provide spatial navigation. The robot arms are moved with proximity sensing to control contact with our cheek surface;
- Investigating how cheek stimulation affects directional guidance. In our experiment on directional guidance, we found that haptic cues on the cheek provided accurate direction two cues in VR space, but that azimuthal angular accuracy was better than elevational one.
- Investigating how cheek stimulation guide users; We experimented on how haptic cues on the cheek improve task performance. In the target searching task, our guidance technique shortens task completion time than only visual information and enhanced spatial directional perception.

2 RELATED WORK

Haptic feedback plays an important role in VR and computer-human interaction. Haptic receptors are distributed throughout the body, while receptors for other major senses: vision, audio, taste, and smell are located in specific facial location. Haptics includes senses for various type of stimuli, such as touch, temperature, and pressure. In previous studies, haptic stimulation has been leveraged to stimulate various body parts and has been integrated other modalities such as visual and audio cues in order to enhance VR experiences as a multi-/cross-modal stimulation.

Our torso has a large surface area. As such, numerous previous studies presented haptic stimuli on this area. Delazio et al. developed a force feedback device that used airbags located on the side of a vest to improve the VR experience [7]. Our hands can be considered as one of the most sensitive regions for haptic stimuli. Günther et al. used a tactile glove that had multiple embedded tactors to navigate 3D space by encoding spatial information into vibration patterns [9]. Chen et al. developed a handheld pin-array haptic display to present a direction to the palm [5]. Ion et al. presented an arm-worn skin drag display to let users recognize a tactile shape [12]. A quadcopter was utilized as a haptic display in 3D space to render a touchable surface [11]. One remarkable system is the wearable robotic arm approach. Shen et al. designed a neck augmentation system using a robotic arm attached to the top of the user's head [21]. AI-Sada et al. developed a wearable robotic arm that provided haptic feedback to a VR user [1]. They attached multiple haptic actuators to the end effector of the arm to enhance the VR experience. However, it was reported that, when the head was not stationary, haptic stimuli to the body were encoded in an eye-centered reference frame [20]. The superiority of the eye-centered frame in directional perception has been reported.

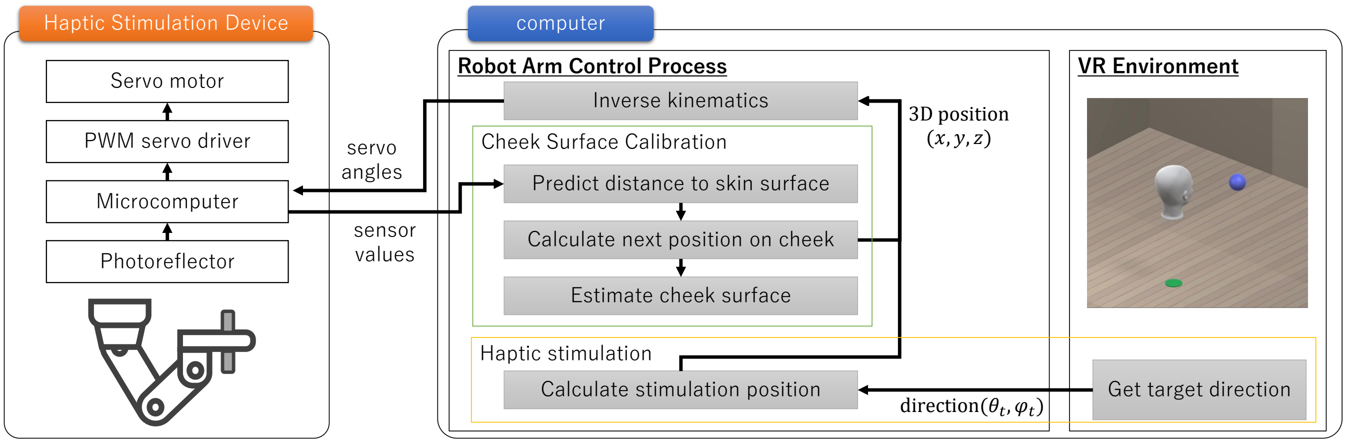

Figure 2: System Configuration

Equally important, our head is another of the most sensitive parts capable of being used for haptic stimuli. So, various interactive haptic devices for the head region have been proposed in previous studies. Tseng et al. attached physical widgets to the HMD to enable tangible interaction [26]. By controlling the widgets physically, they interacted with the virtual environment. Cassinelli et al. built a prototype to detect the surroundings and provide haptic feedback to the head [3]. Berning et al. encoded distance information about the user's surrounding objects into pressure values and presented it to the head, allowing the user to perceive spatial information [2]. Not only 2D- but also 3D- directional interaction techniques have also been proposed. Tsai et al. presented a 2.5D instant impact on an HMD using the impact devices attached to the front side of the HMD [25]. Matsuda et al. developed a necklace-type device to indicate directions via vibration patterns for remote collaboration [17]. Beren et al. placed multiple vibrotactile motors around the head to guide the user even at different heights [14]. Oliveira et al. designed a haptic guidance system with vibrotactile motors around the forehead [6]. They translated the azimuthal direction into vibrational position and the elevational direction into vibrational frequency. Moreover, thermal feedback was leveraged for providing spatial directional cues to the forehead [18, 19]. As the above previous studies indicated, facial haptics is useful for spatial interaction, such as receiving the feedback from the virtual environment, spatial guidance, and spatial awareness.

As a part of the face, the cheek is also sensitive to haptic stimulation, but there are few approaches that leverage it for providing feedback. In the field of brain computer interface, cheek stimuli potential was explored [13]. The cheeks' properties for haptic stimulation were investigated. A previous study showed that in-air ultrasonic haptic cues on the cheek allow users to perceive stimulus location well [8]. Liu et al. found that synchronizing haptic stimulation to the cheek and visual oscillation by user's footstep reduced VR sickness[15]. Theo et al. integrated visual stimulation with the cheek haptic feedback and vestibular stimulation by the electronic current to present weight sensation [24]. The above approaches presented haptic stimulation to specific locations on the cheek, while Wilberz et al. mounted a robot arm to an HMD to provide haptic stimulation around the mouth in fully localizable positions [29]. They attached some actuators to provide multiple haptic feedback and found that users could judge directions from wind cues. They also showed the multi-modal haptic feedback improved the overall VR experience.

Haptic systems are useful for augmenting a human's ability. Primarily, the cheeks and mouth are more sensitive than the other facial areas. Previous studies revealed that the cheek's potential of directional perception was superior to other areas and that fully localizable stimulation improved the VR experience. Most mouth stimulation approaches presented ambient information such as wind [29] and investigated horizontal directional cues. By utilizing cheeks' directional potential, we developed a cheek haptic-based guidance system in 3D space. Lip skin is thin and, as such, susceptible to various damage; direct stimulation to the lips can cause discomfort. Therefore, we explored the potential of haptic feedback to only the cheeks, minus the lips. We investigated how "direct" haptic stimulation to the cheek could guide in 3D space. Also, through our experiments, we investigated how vertical movements on the cheek can guide in the elevational plane. In order to provide haptic cues on cheeks, we developed a robot arm-based haptic stimulation system because the robot arm can stimulate at a free point on the cheeks.

3 SYSTEM DESIGN

We describe the principle of our guidance method. We decide to use the cheeks for presenting directional cues to an HMD user. Our face has a dense distribution of haptic receptors as indicated in Penfield's homunculus. Especially, the mouth and cheeks are sensitive to mechanical stimuli, so we can recognize the stimulation position precisely. However, our lips are more susceptible to even slight stimulation due to their thin skin layer. In addition, the lip engages in essential activities such as eating and speaking. Therefore, we avoid stimulating the lip. Strong force toward the teeth can injure the mouth because of the teeth's hardness. Therefore, we touch both sides of the cheeks with weak to moderate force.

For stimulating the cheek, we attach two robotic arms to an HMD. We can recognize the stimulation position on the cheek, and

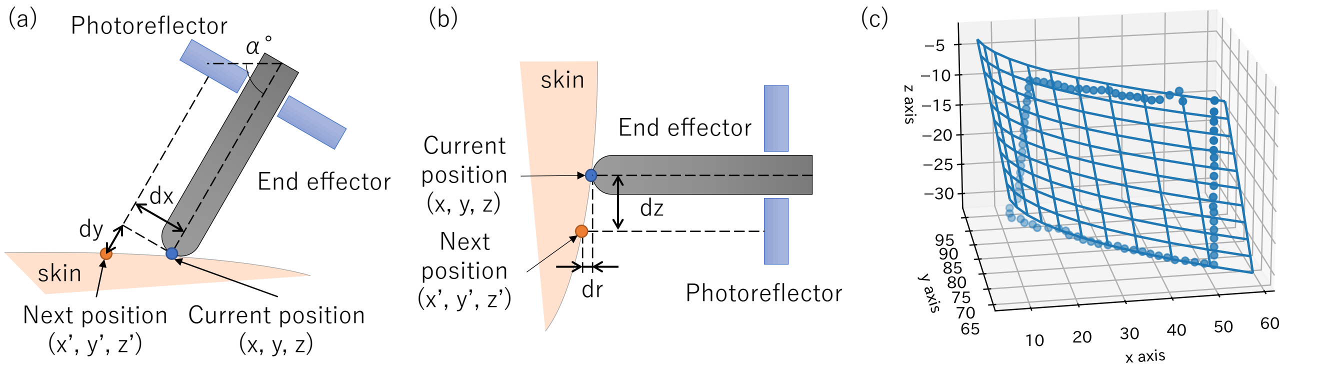

Figure 3: Cheek surface calibration. Left: Cheek surface tracking in horizontal direction. Center: Cheek surface tracking in vertical direction. Right: Fitted quadratic surface to 3D points on cheek surface. Blue markers were the actual points on the cheek surface. Wireframe was estimated surface.

a haptic device that can stimulate the precise position is required. So, we utilize a robot arm with some linkage so that the arm can stimulate a localizable position on the cheek. We attach the robot arms to an HMD to present the stimulation even while walking around. However, if only one robot arm is used, it increases the overall weight because it requires a linkage extension and high-torque motors for the joint. Therefore, we employ two robot arms for stimulating the left and right sides of the cheeks.

When touching the cheek with the robot arms, the surface geometry information of the cheek is required. A camera-based approach is popular for measuring facial geometry. However, an HMD and a robot arm can occlude the face. When a camera is mounted on the robot arm, the sensing would be difficult because of a motion blur. Therefore, we use photoreflectors as proximity sensors. A Photoreflector has a light emitting diode and a phototransistor. A light emitting diode emits the light, and a phototransistor detects the intensity of the light reflected from a skin surface. The light intensity varies with the distance between the photoreflector and the object, so the phototransistor value can be converted to a distance. Photoreflectors can detect the distance in a close range, so we attach them to the end effector of the arms. On each four sides of the end effector, a photoreflector is arranged to detect the distance to the skin surface so that the shape around the end effector can be obtained. Photoreflectors detect points on the cheek surface and track the cheek surface (Fig. 3). Thus, we collect the points on the cheek surface. We assume that this local facial part can be represented as a quadratic surface. We fit the quadratic surface to the points on the cheek in order to obtain the cheek surface.

When presenting the haptic stimulation indicated a target direction, we need to map the direction to a point on the cheek (Fig. 5). We get the target direction (azimuthal and elevational angle) by converting the Cartesian coordinate system to a spherical coordinate system. The azimuthal and elevational angles are transformed into a line equation. The elevational angle is converted to an offset of the height position, and the azimuthal angle is converted to the slope of the line. We calculated an intersection between the quadratic cheek surface and the direction represented as the line. We use this intersection as a stimulation point. However, we cannot present the frontal direction because we avoid touching our lips, which are located on the center of our face. Therefore, we used two robot arms to stimulate both cheeks at the same time when the target positions in front of the user. Thus, we present a directional cue by touching on the position corresponding to the spatial information of the target.

4 IMPLEMENTATION

We developed a system to provide directional cues on the cheek (Fig. 2). Our system consisted of a haptic stimulation device (Fig. 4) and software. The device presents haptic directional cues on the cheek using two robotic arms. We described the details of the device in Section 4.1. The software controlled robot arms, detected the cheek surface, translated a direction to a point on the cheek. We integrated software and hardware to VE developed with Unity. These functions were described in Section 4.2, Section 4.3, and Section 4.4 respectively.

4.1 Haptic Stimulation Device

We built a haptic stimulation device by modifying an Oculus Rift CV1 (Fig. 4). We attached two robotic arms and a circuit. The robotic arms were attached to the left and right sides of the bottom of the HMD so that they stimulated each side of the cheeks. We fixed the robotic arms by using brackets created with a 3D printer. The circuit was attached to the HMD's head strap and mounted on the top of the HMD.

The robotic arm was designed with 5 DoF (degree of freedom), allowing to stimulate the cheek in 3D space. We used five servo motors (SG-90, Tower Pro) on the joints for each robot arm and placed one at each joint. The tip of the arm was rounded to avoid hurting the cheeks. The end effector had four photoreflectors on the right, left, up, and down sides (Fig. 4).

The circuit had a microcomputer (Arduino Nano) and a pulse width modulation (PWM) servo driver (PCA9685, NXP). The microcomputer was connected to a USB cable. The microcomputer received instructions from the software via serial communication, rotated servo motors, and sent sensor values of photoreflectors. The microcomputer communicated the PWM servo driver with I2C.

The servo driver control servo rotation. Servo motors supplied the power by 5V AC adapter. The microcomputer got photoreflector values via an analog multiplexer (TC4052BP, TOSHIBA). The microcomputer was fixed to a bracket created by a 3D printer and attached to the top of HMD through the headset strap. The cables were covered by black tubes.

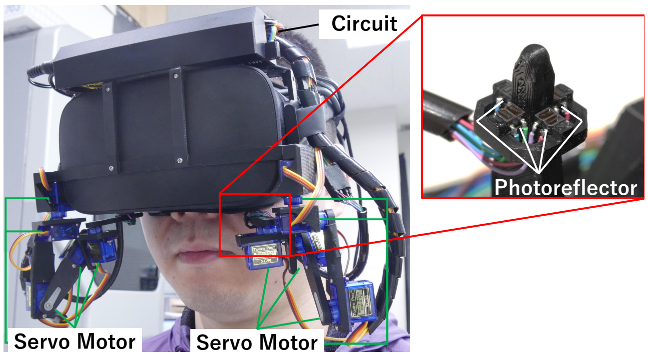

Figure 4: Haptic Stimulation Device

4.2 Robot Arm Control

We utilized inverse kinematics to move the robot arms to a localized 3D position. Inverse Kinematics solved the servo angles of each joint of the arms from a 3D position. The robot arms were moved by rotating servo motors to the calculated angles. However, when measuring the cheek surface, the end effector was faced in various directions so that the photoreflectors could not detect the skin surface. Therefore, we controlled the end effector to keep its angle constant. Two servo motors employed to rotate the tip, one to keep the azimuth angle at 60 degrees and the other to keep the elevation angle horizontal to the ground. These angles were decided empirically. We defined the origin in robot arm coordinate as the first joint of the arm.

4.3 Cheek Surface Detection

We calibrated the mapping between real and VR space to encode a virtual target into the position on the cheek surface. For the cheek surface calibration, the 3D points on the cheek surface were detected and collected. By fitting a quadratic surface to the collected 3D points, we estimated the cheek surfaces. Calibration was performed for each arm because of the asymmetry of the facial geometry. Also, we set only the width and height of the stimulation area because the facial geometry depends on each person.

In collecting the point on the cheek surface, each robot arm traced the edge of a rectangular area for stimulation. At first, the robot arm touched the cheek surface in a straight line from the initial position. While the arm is moving, the photoreflectors measured the distance from the arm tip to the cheek surface and converted the sensor values into a distance in the real world with a linear regression model. Then, the arm moved along the cheek edge of the stimulation area in the left, down, right, and up directions in sequence. When the arm moved to the left, a photoreflector on the left side of the arm tip measured the distance to the cheek surface and our system computed a point on left side of the arm tip with formula 1 (Fig. 3, left).

$$\begin{pmatrix} x' \\ y' \\ z' \end{pmatrix} = \begin{pmatrix} x \\ y \\ z \end{pmatrix} + \begin{pmatrix} -\sin\alpha & \cos\alpha & 0 \\ \cos\alpha & \sin\alpha & 0 \\ 0 & 0 & 1 \end{pmatrix} \begin{pmatrix} dx \\ dy \\ 0 \end{pmatrix} \tag{1}$$

dx was 1.5 because the photoreflector width was about 3.0mm, and α was 60 degree as described in Section 4.1. The arm iterated to move the detected point until the arm reached the left edge of the stimulation area. When the arm moved down, a photoreflector located on the bottom side of the arm tip measured the distance to the cheek surface, and our system calculated the position of a point on the lower side of the arm tip using formula 2 (Fig. 3, center).

$$\begin{pmatrix} x' \\ y' \\ z' \end{pmatrix} = \begin{pmatrix} x \\ y \\ z \end{pmatrix} + \begin{pmatrix} \cos\beta & -\sin\beta & 0 \\ \sin\beta & \cos\beta & 0 \\ 0 & 0 & 1 \end{pmatrix} \begin{pmatrix} 0 \\ dr \\ dz \end{pmatrix} \tag{2}$$

dz was decided to 1.5 thanks to the photoreflector width, and β was the angle of first joint of the arm. The arm iterated to move the detected point until the arm reached the bottom edge of the stimulation area. A similar procedure as above was performed when the arm moved to the right and up direction. Thus, the arm moved on the stimulation area. By gathering the points of the arm trajectory, we acquired 3D points of the cheek surface.

We estimated the cheek surface by fitting a quadratic surface to collected 3D points (Fig. 3, right). We fitted the quadratic surface to collected points to compute the parameters of the quadratic surface with least-square method (equation 3). This way, we obtained the cheek surface as the quadratic surface. The cheek surfaces were estimated for both left and right arms, and each side of the surface was estimated separately.

$$ax^2 + by^2 + cx + dy + e = z \tag{3}$$

4.4 Haptic Stimulation

We presented the haptic directional cues with the robotic arm, changing the stimulation according to the spatial information of the target (Fig. 5). We obtained directional information from the target position (x_t, y_t, z_t) and computed the corresponding cheek position (x_s, y_s, z_s). Based on the cheek position (x_s, y_s, z_s), we determined the position (x_c, y_c, z_c) and the method of the cheek stimulation.

In calculating the point on the cheek (x_s, y_s, z_s) corresponding to the target's position (x_t, y_t, z_t), we converted the position information into directional information in VR space. The target's position (x_t, y_t, z_t) was converted to the position from user's view (x_{tu}, y_{tu}, z_{tu}). By converting the position in Cartesian coordinate (x_{tu}, y_{tu}, z_{tu}) to the position in Spherical coordinate $(r_t, \theta_t, \varphi_t)$, an azimuthal angle φ_t and an elevation angle θ_t were calculated. We mapped the azimuthal and elevation angle (φ_t, θ_t) to the point on a curved surface (x_s, y_s, z_s). The sine of the elevation angle θ_t was mapped to the height of the cheek coordinates z_{offset} (formula 4).

$$z_{offset} = \begin{cases} z_{min} & (\theta_t < 0) \\ \frac{\sin\theta_t}{\sin\theta_{max}} * (z_{max} - z_{min}) & (0 \le \theta_t < \theta_{max}) \\ z_{max} & (\theta_t \ge \theta_{max}) \end{cases} \tag{4}$$

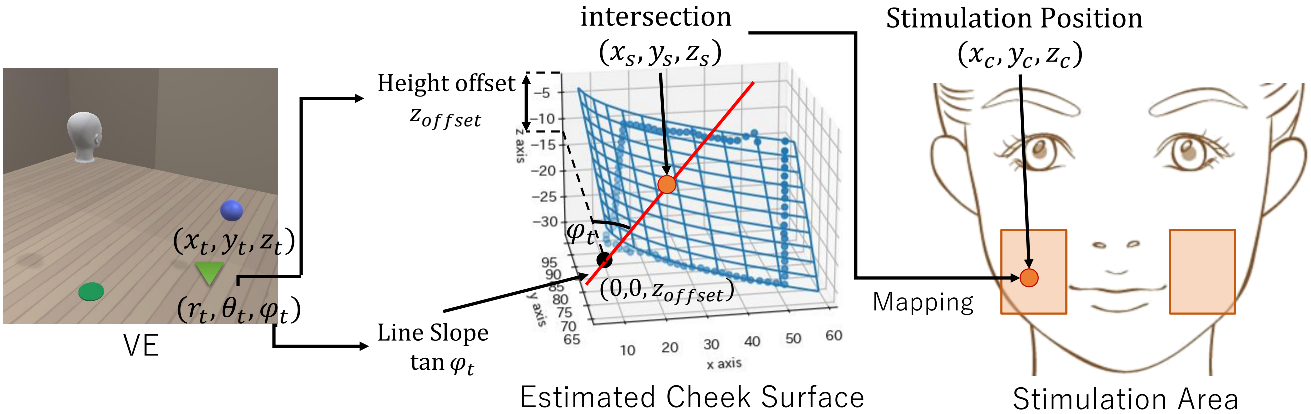

Figure 5: Haptic stimulation flow. The target position was converted to an azimuthal and an elevational angle. These two angles were translated into a line. The intersection between the line and the cheek surface was calculated and was mapped to the stimulation area (transparent orange area) to obtain the stimulation position.

In our implementation, θ_{max} was 45 degrees, z_{min} was 0, and z_{max} was 30. The azimuthal angle φ_t was translated to a line representation and added the height offset z_{offset} (formula 5, t is constant).

$$\begin{pmatrix} x \\ y \\ z \end{pmatrix} = t \begin{pmatrix} \tan \varphi_t \\ 1 \\ 0 \end{pmatrix} + \begin{pmatrix} 0 \\ 0 \\ z_{offset} \end{pmatrix} \tag{5}$$

We computed the intersection between the estimated cheek surface (formula 3) and the line (formula 5). In this way, we calculated the cheek position (x_s, y_s, z_s) that mapped to the target position in VR space (x_t, y_t, z_t).

Since the calculated point (x_s, y_s, z_s) could be out of the stimulation area, we decided the stimulation method and the stimulation position (x_c, y_c, z_c) based on x_s. x_s was classified into four areas; area A was $x_f < x_s$; area B was $x_{c_{max}} \le x_s < x_f$; area C was $x_{c_{min}} \le x_s \le x_{c_{max}}$; area D was $x_s < x_{c_{min}}$. x_f was the threshold of the facial center area. $x_{c_{max}}$ and $x_{c_{min}}$ were the maximum and minimum value of the stimulus range respectively. Based on which area x_s was, we calculated the stimulation position as follows:

$$(x_c, y_c, z_c) = \begin{cases} (x_{c_{max}}, y_{x_{c_{max}}, z_s}, z_s) & (x_s \text{ in area A or B}) \\ (x_s, y_{x_s}, z_s) & (x_s \text{ in area C}) \\ (x_{c_{min}}, y_{x_{c_{min}}, z_s}, z_s) & (x_s \text{ in area D}) \end{cases} \tag{6}$$

$y_{x_{c_{max}}, z_s}$ was the y value in equation 3 when $x = x_{c_{max}}$ and $z = z_s$. $y_{x_{c_{min}}, z_s}$ was the y value in equation 3 when $x = x_{c_{max}}$ and $z = z_s$. If x_s was in area A, we used both arms for the stimulation and calculated the stimulation positions on both sides. If not, we used one robot arm. The stimulus of azimuthal direction was discrete, but that of elevational direction was continuous. We expected the continuous stimulation in the elevational plane would help users to recognize the height information accurately. Finally, we decided the stimulation position (x_c, y_c, z_c) and touched it with the robot arms.

5 EXPERIMENT1: DIRECTIONAL GUIDANCE

We investigated how haptic cues on the cheeks provided directional information in VR space. In this experiment, participants looked for and pointed the invisible target in 3D space with haptic cues on cheeks. The targets appeared at fifteen-degree intervals of 180 degrees in the azimuthal plane and of 90 degrees in the elevation plane, so the appeared location was totally 91 (13 (azimuth) * 7 (elevation)). When the target appeared, the robot arms began to stimulate the participant's cheeks. The stimulation was provided depending on the gap between the participant's direction and the target direction. In the VR system, the only head rotation was reflected, while the head position was fixed. Participants pointed the position by turning to the target direction and by pressing a controller button. We placed a reticle in front of participants to help them to select the target. We showed instruction texts to participants in the VR space. We evaluated the absolute azimuthal and the absolute elevational angular error and task completion time. There were six participants (six males; age was M=23.5, SD=0.96), and they had no disability related to tactile organs. All participants had experienced using VR (> 10 times), and two of them played VR less than an hour a week and the rest of them played VR more than an hour a week.

Our experiment had two sessions, namely, a rehearsal session and an actual performance session. In the rehearsal session, participants looked for the target with visual and haptic feedback. The rehearsal session had 45 trials, and one target appeared in each trial. We set a five seconds interval between each trial. Participants were instructed to look at the front during the intervals. During the intervals, the stimulation stopped and the robot arms returned to the initial position. When participants selected the correct target, they heard the audio feedback for the correct answer. In the actual performance session, participants searched the invisible target with haptic feedback. The session had 91 trials. When participants selected the direction, they heard the audio feedback. We instructed the participants to wear earplugs and a noise canceling headphone and let the participant hear white noise during the experiment to

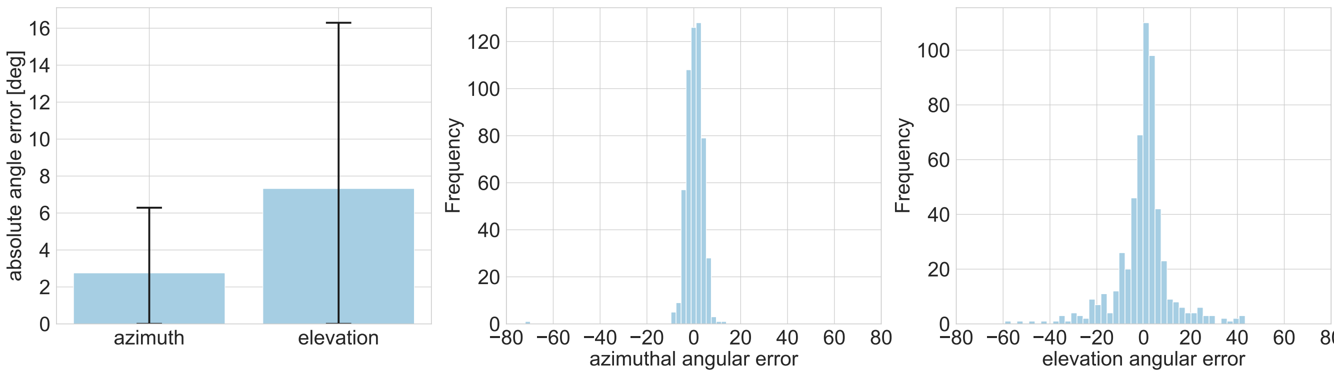

Figure 6: The result of directional guidance pointing accuracy. Left: absolute azimuthal and absolute elevational angular error. Center: a histogram of azimuthal angular error. A bar width indicated the four degree. Right: a histogram of elevational angular error. A bar width indicated the four degree.

reduce the noise from robot arms and to hear only the sound from the VE.

5.1 Experimental Protocol

We first explained the task and the procedure of the experiment to the participants. We instructed the participant to put on the device and earplugs and sit him on a chair. Then, we calibrated the cheek surface of the participant. We instructed the participant not to move during the calibration. After calibration, we displayed a VE and presented visual and haptic information of the target position to the participant. Here, we instructed the participant to move the head up, down, left, and right to demonstrate haptic stimulation when the target was located in front. After the demonstration, we put a noise canceling headphone on the participant and the rehearsal session started. In the rehearsal session, the participant searched for the visible target 45 times. Immediately after the rehearsal session, an actual performance session started. In the actual performance session, the participant searched for the invisible target 91 times. After the actual performance session, the participant removed the earplugs, the headphone, and the device. The participants sit to the seat during the experiment.

5.2 Result

The result is shown in Fig. 6. The absolute azimuthal angular error was M=2.76 degrees, SD=3.53 degrees. On the other hand, the absolute elevation angular error was M=7.32 degrees, SD=8.97 degrees (Fig. 6 (Left)). The task completion time was M=7.42 seconds, SD=7.64 seconds. Also, we plotted histograms of both angular error respectively (Fig. 6 (Center, Right)). We showed an example of temporal changes of the gap between the target direction and head one (Fig. 7). According to the histograms of both directions, almost azimuthal angular errors were around 10 degrees. It is because we stimulated both cheeks when the target was within 10 degrees of the azimuthal angle in our implementation.

On the other hand, elevation angular error was larger than azimuthal one. We expected the elevation error was similar to the azimuthal one because we provided continuous stimulation on the cheek as described in Section 4.4. However, it seemed to be difficult

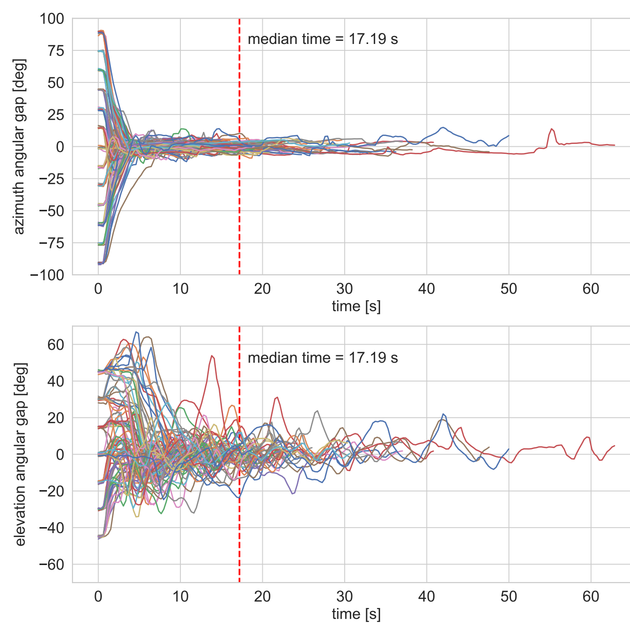

Figure 7: Example of temporal change of azimuthal and elevation angular gap between the center point of a participant view and target position in Experiment 1. These contained 91 trials. The red line indicated a median of task completion time.

to recognize the elevation angle as the result showed. As shown in Fig. 7, the participants repeatedly shook their heads in elevational direction. After the experiment, all participants reported that they had difficulty finding the elevational direction. Furthermore, one participant reported that he lost the origin of height direction of haptic feedback during the experiment. We considered that our feedback of elevational direction has room for improvement, as the simple continuous feedback could result in ambiguity.

After the experiment, some participants mentioned that they sometimes did not feel the haptic feedback. This was caused by a slight change in the position of the device as the participant moved the head. In our system, the robot arms were fixed to the HMD, so when the HMD moved, the distance to the cheek also changed. When the participants looked down, the HMD could move due to the effect of gravity. Therefore, a method to adaptively estimate the cheek surface is required.

6 EXPERIMENT 2: SPATIAL GUIDANCE

We investigated how our spatial guidance technique was effective in VR space. Participants had to look for and touch the visible target in 3D space. We compared task completion time in visual + haptic condition with in visual condition. In visual condition, participants searched the target with only visual information. In the visual + haptic condition, participants detected the target with visual information and haptic feedback to cheeks. There were six participants (six males; age was M=23.5, SD=0.96), and they had no disability related to tactile organs and vision. All participants had experienced using VR (> 10 times), and two of them played VR less than an hour a week and the rest of them played VR more than an hour a week.

Participants searched for and found targets of a specific color among several spheres. Participants performed 80 trials and took a break after every 20 trials. Each target ball was placed in a room (3 m x 3 m x 2 m) with 50 balls in it. The target positions were placed in randomly chosen positions. The target positions were used to generate 40 random locations and then randomly sorted to generate a set of counterbalanced positions totaling 80 points. The other 49 fakes were randomly placed at the beginning of each trial. In this case, each ball was placed so that they did not overlap. The colors of the targets and fakes were randomly set when the trial started. The color of each ball was set so that the distance between its colors in HSV space was greater than 0.25. When the balls appeared, the robot arms began to stimulate the participant's cheeks. The stimulation was provided depending on the gap between the participant's direction and the target direction. In this experiment, the position and rotation of the head were reflected in the VR environment. The example of the room for the experimfent is shown in Fig 8.

6.1 Experiment Protocol

Our experiment had two sessions, namely, a rehearsal session, an actual performance session. Before the actual performance session, we let participants train to find the target in each condition. In the rehearsal session, participants looked for the target with each condition. The session had 20 trials and one target appeared in each trial. There was a 5 seconds interval between each trial. During the interval, the cheek stimulation stopped and the robot arms returned to their initial position. Participants were instructed to look in front of them while waiting for the next trial. When participants selected the correct target, they heard the audio feedback for the correct answer. In the actual performance session, participants searched the visible target with haptic feedback. The session had 80 trials and the participants took a break after every 20 trials. We instructed the procedure to the participants before the experiment.

We showed this experiment flow below:

(1) The participant was instructed to go to the center of the room. The center was indicated as a circle.

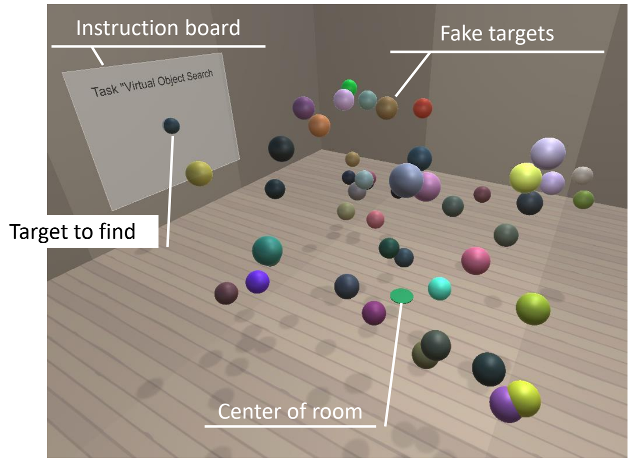

Figure 8: Virtual Environment of Experiment 2

(2) The participant was shown the target to find and was heard a sound.
(3) The participant looked for the target. The target to find was located in the front of participants.
(4) When the participant touched the target, the trial was finished.

6.2 Result

The overall average result is shown in Fig. 9 and the individual results are shown in Fig. 10. The task completion time in visual condition was M=12.45 s, SD = 14.51 s. The task completion time in visual and haptic condition was M = 6.91 s, 5.48 s. Friedman test revealed that there was a significant difference (p=0.014) between visual condition and visual+haptic condition in terms of the task completion time.

Looking at the participants' behavior during the experiment, the Visual+Haptic condition resulted in faster behavior when exploring. However, the search took longer when the target was at the foot of or above the target. In the Visual + Haptic condition, participants searched horizontally from their field of view first, and therefore could not locate the target located under their feet. They acted like he was looking around, so they were able to find them quickly. This is because the azimuthal direction was the easiest to find in our direction presentation. We also found that users were confused when searching for targets, even when the targets seemed to be hidden by fakes in the eyes of the participants. Since our system does not present information about the depth direction, this may be because we felt an inconsistency between the visual and haptic information when occlusion occurs.

After the experiment, some participants reported that they changed their behavior in the Visual and Visual+Haptic conditions. In the Visual condition, the participants learned the target's color without making mistakes, but in the Visual+Haptic condition, they learned the rough color of the target and looked for it by haptic stimulation. This is because the Visual condition provided no directional information and some colors were difficult to identify, while the Visual+Haptic condition provided directional cues. Also, in the

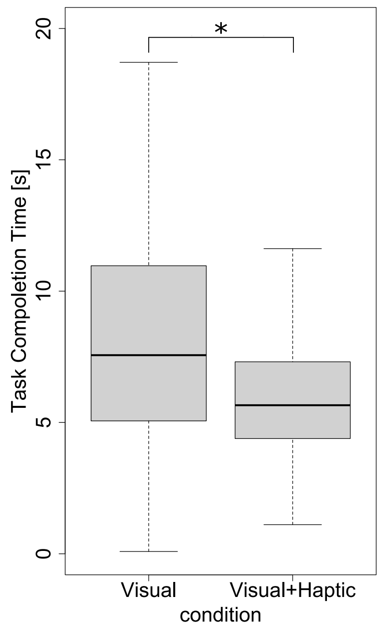

Figure 9: Box Plot of Task Completion Time in Visual and Visual+Haptic condition

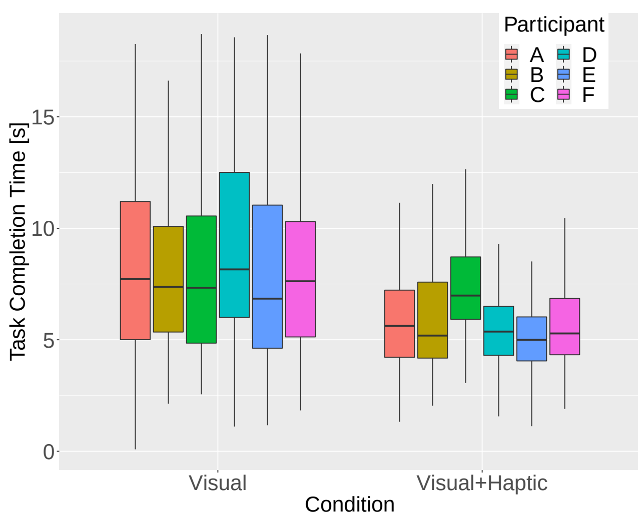

Figure 10: Box plot of Task Completion Time in Each Condition for Each Participant

Visual+Haptic condition, some participants did not feel the stimulation when they changed their facial expressions after successfully locating the target. This is an issue with our haptic presentation method using cheek surface estimation. We calibrated only once before stimulating the cheek surface and did not do so afterwards. However, the cheeks change their facial shape, such as when making facial expressions. Especially in the region near the lips, the haptic stimulation seemed to disappear because the tactile stimulus position was around there when the target was in front.

7 LIMITATION

Our technique could present an object's direction by estimating the surface as static and providing the stimulus to the cheek. However, the cheeks deform dynamically when speaking, eating, and forming facial expressions. Therefore, it is difficult for the current implementation to cope with physiological deformations of the cheeks due to physiological reactions. Not only that, but it is also difficult for users to wear the HMD in exactly the same position every time. A similar issue has been shown in previous studies on photo-reflector-based sensing, and it is necessary to deal with this misalignment between the HMD and face. Therefore, it is essential to build a robust cheek sensing method accounting for the dynamic deformation of the cheek and displacement of the HMD.

We employed a servo motor for the robot arm. The angular step of this servo motor was 1.8 degrees and its PWM control width was 20 ms. In the future, we will test whether directional presentation can be made more accurate and rapid by the arm using a high resolution servo to improve the accuracy of the stimuli by the arm, both in time and space.

We leveraged a robotic arm with a linkage mechanism as a stimulation device. However, the arm with a linkage mechanism requires multiple joints, and a servo arm needs to be attached to the linkage, which increases the weight of the arm. This weight increase makes the users tired. Therefore, it is necessary to construct a lightweight robot arm.

As shown in the result of experiment 1, the elevational angular error was larger than the azimuthal one. While participants seemed to have difficulty in moving their heads slightly, there is a possibility that the limitation of our robot arm-based haptic stimulation led to this result. However, there was no means of investigating how precisely a human can move in the elevational direction by themselves. In the future, we will investigate the controllable angle of the human head.

It is generally known that continuous haptic stimulation can lose the sensation by sensory adaptation, while the participants did not mention that in our experiments. We will investigate if such adaptation occurs when stimulating the cheek with our method for a longer duration.

8 CONCLUSION

We developed Virtual Whiskers, a spatial directional guidance system that offered haptic cues to the cheeks by using robot arms attached to an HMD. We attached robotic arms to the left and right sides of the bottom of an HMD, allowing to provide haptic cues on both cheeks. Our system detected points on the cheeks' surface using photo reflective sensors located on the tip of robot arms and estimated the cheek surface by fitting a quadratic surface to the points. When the arms touched the cheeks, we calculated the point on the estimated surface corresponding to azimuthal and elevational angles of the target in VR space. Depending on the position, we touched the cheeks with the arms to offer directional cues.

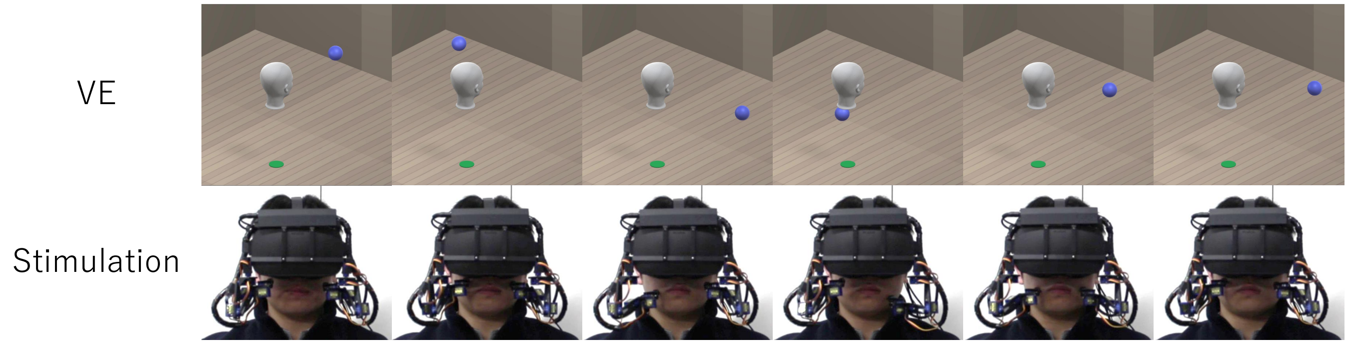

Figure 11: Haptic directional cue presentation with robot arm attached to the HMD. The upper row was the VE. The 3D head model was the user's head position. The blue sphere was a target. The bottom row was the user that stimulated the cheek with the robot arms attached to the HMD.

We experimented the directional guidance accuracy by haptic directional cues on the cheeks and evaluated the pointing accuracy. Our method achieved the absolute azimuthal pointing error of M=2.76 degrees, SD=3.53 degrees and the absolute elevational absolute pointing error of M=7.32 degrees, SD=8.97 degrees. We also experimented a task performance in spatial guidance task with our guidance technique. We compared the task completion time in the target finding task in the condition that only visual information was presented and in the condition that visual and haptic information was presented. The result showed that the average of task completion time in the visual condition was M=12.45 s, SD = 14.51 s and of the in visual and haptic condition was M = 6.91 s, 5.48 s. Statistical test showed a significant difference in task completion time between the visual condition and visual+haptic condition.

In this paper, we presented a single direction by stimulating the cheek with two robotic arms. However, several robotic arms can be leveraged for the interaction with several virtual objects. In the future, we will explore the potential application and the interaction method of virtual objects.

ACKNOWLEDGMENTS

This project was supported by JST ERATO Grant Number JPMJER1701 and JSPS KAKENHI Grant Number 16H05870.

REFERENCES

[1] Mohammed Al-Sada, Keren Jiang, Shubhankar Ranade, Mohammed Kalkattawi, and Tatsuo Nakajima. 2020. HapticSnakes: multi-haptic feedback wearable robots for immersive virtual reality. *Virtual Reality* 24, 2 (2020), 191–209.

[2] Matthias Berning, Florian Braun, Till Riedel, and Michael Beigl. 2015. ProximityHat: A Head-Worn System for Subtle Sensory Augmentation with Tactile Stimulation. In *Proceedings of the 2015 ACM International Symposium on Wearable Computers* (Osaka, Japan) *(ISWC '15)*. Association for Computing Machinery, New York, NY, USA, 31–38. https://doi.org/10.1145/2802083.2802088

[3] Alvaro Cassinelli, Carson Reynolds, and Masatoshi Ishikawa. 2006. Augmenting spatial awareness with Haptic Radar. In *2006 10th IEEE International Symposium on Wearable Computers*. 61–64. https://doi.org/10.1109/ISWC.2006.286344

[4] Daniel K.Y. Chen, Jean-Baptiste Chossat, and Peter B. Shull. 2019. HaptiVec. In *Proceedings of the 2019 CHI Conference on Human Factors in Computing Systems - CHI '19*. ACM Press, New York, New York, USA, 1–11. https://doi.org/10.1145/3290605.3300401

[5] Daniel K.Y. Chen, Jean-Baptiste Chossat, and Peter B. Shull. 2019. HaptiVec: Presenting Haptic Feedback Vectors in Handheld Controllers Using Embedded Tactile Pin Arrays. In *Proceedings of the 2019 CHI Conference on Human Factors in Computing Systems* (Glasgow, Scotland Uk) *(CHI '19)*. Association for Computing Machinery, New York, NY, USA, 1–11. https://doi.org/10.1145/3290605.3300401

[6] Victor Adriel de Jesus Oliveira, Luca Brayda, Luciana Nedel, and Anderson Maciel. 2017. Designing a Vibrotactile Head-Mounted Display for Spatial Awareness in 3D Spaces. *IEEE Transactions on Visualization and Computer Graphics* 23, 4 (April 2017), 1409–1417. https://doi.org/10.1109/TVCG.2017.2657238

[7] Alexandra Delazio, Ken Nakagaki, Roberta L. Klatzky, Scott E. Hudson, Jill Fain Lehman, and Alanson P. Sample. 2018. Force Jacket: Pneumatically-Actuated Jacket for Embodied Haptic Experiences. In *Proceedings of the 2018 CHI Conference on Human Factors in Computing Systems* (Montreal QC, Canada) *(CHI '18)*. Association for Computing Machinery, New York, NY, USA, 1–12. https://doi.org/10.1145/3173574.3173894

[8] Hyunjae Gil, Hyungki Son, Jin Ryong Kim, and Ian Oakley. 2018. Whiskers: Exploring the Use of Ultrasonic Haptic Cues on the Face. In *Proceedings of the 2018 CHI Conference on Human Factors in Computing Systems* (Montreal QC, Canada) *(CHI '18)*. Association for Computing Machinery, New York, NY, USA, 1–13. https://doi.org/10.1145/3173574.3174232

[9] Sebastian Günther, Florian Müller, Markus Funk, Jan Kirchner, Niloofar Dezfuli, and Max Mühlhäuser. 2018. TactileGlove: Assistive Spatial Guidance in 3D Space through Vibrotactile Navigation. In *Proceedings of the 11th PErvasive Technologies Related to Assistive Environments Conference* (Corfu, Greece) *(PETRA '18)*. Association for Computing Machinery, New York, NY, USA, 273–280. https://doi.org/10.1145/3197768.3197785

[10] Cristy Ho and Charles Spence. 2007. Head orientation biases tactile localization. *Brain research* 1144 (2007), 136–141.

[11] Matthias Hoppe, Pascal Knierim, Thomas Kosch, Markus Funk, Lauren Futami, Stefan Schneegass, Niels Henze, Albrecht Schmidt, and Tonja Machulla. 2018. VRHapticDrones: Providing Haptics in Virtual Reality through Quadcopters. In *Proceedings of the 17th International Conference on Mobile and Ubiquitous Multimedia* (Cairo, Egypt) *(MUM 2018)*. Association for Computing Machinery, New York, NY, USA, 7–18. https://doi.org/10.1145/3282894.3282898

[12] Alexandra Ion, Edward Jay Wang, and Patrick Baudisch. 2015. *Skin Drag Displays: Dragging a Physical Tactor across the User's Skin Produces a Stronger Tactile Stimulus than Vibrotactile.* Association for Computing Machinery, New York, NY, USA, 2501–2504. https://doi.org/10.1145/2702123.2702459

[13] J. Jin, Z. Chen, R. Xu, Y. Miao, X. Wang, and T. P. Jung. 2020. Developing a Novel Tactile P300 Brain-Computer Interface With a Cheeks-Stim Paradigm. *IEEE Transactions on Biomedical Engineering* 67, 9 (2020), 2585–2593. https://doi.org/10.1109/TBME.2020.2965178

[14] Oliver Beren Kaul and Michael Rohs. 2017. HapticHead: A Spherical Vibrotactile Grid around the Head for 3D Guidance in Virtual and Augmented Reality. In *Proceedings of the 2017 CHI Conference on Human Factors in Computing Systems* (Denver, Colorado, USA) *(CHI '17)*. Association for Computing Machinery, New York, NY, USA, 3729–3740. https://doi.org/10.1145/3025453.3025684

[15] S. Liu, N. Yu, L. Chan, Y. Peng, W. Sun, and M. Y. Chen. 2019. PhantomLegs: Reducing Virtual Reality Sickness Using Head-Worn Haptic Devices. In *2019 IEEE Conference on Virtual Reality and 3D User Interfaces (VR)*. 817–826. https://doi.org/10.1109/VR.2019.8798158

[16] Joost X. Maier and Jennifer M. Groh. 2009. Multisensory guidance of orienting behavior. *Hearing Research* 258, 1-2 (dec 2009), 106–112. https://doi.org/10.1016/j.heares.2009.05.008

[17] Akira Matsuda, Kazunori Nozawa, Kazuki Takata, Atsushi Izumihara, and Jun Rekimoto. 2020. HapticPointer: A Neck-Worn Device That Presents Direction by Vibrotactile Feedback for Remote Collaboration Tasks. In *Proceedings of the Augmented Humans International Conference* (Kaiserslautern, Germany) *(AHs '20)*. Association for Computing Machinery, New York, NY, USA, Article 7, 10 pages.

https://doi.org/10.1145/3384657.3384777

[18] Roshan Lalintha Peiris, Wei Peng, Zikun Chen, Liwei Chan, and Kouta Minamizawa. 2017. *ThermoVR: Exploring Integrated Thermal Haptic Feedback with Head Mounted Displays.* Association for Computing Machinery, New York, NY, USA, 5452–5456. https://doi.org/10.1145/3025453.3025824

[19] R. L. Peiris, W. Peng, Z. Chen, and K. Minamizawa. 2017. Exploration of cuing methods for localization of spatial cues using thermal haptic feedback on the forehead. In *2017 IEEE World Haptics Conference (WHC)*. 400–405. https://doi.org/10.1109/WHC.2017.7989935

[20] Lisa M Pritchett, Michael J Carnevale, and Laurence R Harris. 2012. Reference frames for coding touch location depend on the task. *Experimental brain research* 222, 4 (2012), 437–445.

[21] Lichao Shen, MHD Yamen Saraiji, Kai Kunze, Kouta Minamizawa, and Roshan Lalintha Peiris. 2020. *Visuomotor Influence of Attached Robotic Neck Augmentation.* Association for Computing Machinery, New York, NY, USA. https://doi.org/10.1145/3385959.3418460

[22] Maria Z Siemionow. 2011. *The Know-How of Face Transplantation.* Springer London, London. https://doi.org/10.1007/978-0-85729-253-7

[23] Alan F. Stokes and Christopher D. Wickens. 1988. Aviation Displays. In *Human Factors in Aviation.* Elsevier, 387–431. https://doi.org/10.1016/B978-0-08-057090-7.50018-7

[24] Theophilus Teo, Fumihiko Nakamura, Maki Sugimoto, Adrien Verhulst, Gun A. Lee, Mark Billinghurst, and Matt Adcock. 2020. WeightSync: Proprioceptive and Haptic Stimulation for Virtual Physical Perception. In *ICAT-EGVE 2020 - International Conference on Artificial Reality and Telexistence and Eurographics Symposium on Virtual Environments*, Ferran Argelaguet, Ryan McMahan, and Maki Sugimoto (Eds.). The Eurographics Association. https://doi.org/10.2312/egve.20201253

[25] Hsin-Ruey Tsai and Bing-Yu Chen. 2019. ElastImpact: 2.5D Multilevel Instant Impact Using Elasticity on Head-Mounted Displays. In *Proceedings of the 32nd Annual ACM Symposium on User Interface Software and Technology* (New Orleans, LA, USA) *(UIST '19)*. Association for Computing Machinery, New York, NY, USA, 429–437. https://doi.org/10.1145/3332165.3347931

[26] Wen-Jie Tseng, Li-Yang Wang, and Liwei Chan. 2019. FaceWidgets: Exploring Tangible Interaction on Face with Head-Mounted Displays. In *Proceedings of the 32nd Annual ACM Symposium on User Interface Software and Technology* (New Orleans, LA, USA) *(UIST '19)*. Association for Computing Machinery, New York, NY, USA, 417–427. https://doi.org/10.1145/3332165.3347946

[27] Jan BF Van Erp. 2005. Presenting directions with a vibrotactile torso display. *Ergonomics* 48, 3 (2005), 302–313.

[28] Bernhard Weber, Simon Schätzle, Thomas Hulin, Carsten Preusche, and Barbara Deml. 2011. Evaluation of a vibrotactile feedback device for spatial guidance. *2011 IEEE World Haptics Conference, WHC 2011* (2011), 349–354. https://doi.org/10.1109/WHC.2011.5945511

[29] Alexander Wilberz, Dominik Leschtschow, Christina Trepkowski, Jens Maiero, Ernst Kruijff, and Bernhard Riecke. 2020. FaceHaptics: Robot Arm Based Versatile Facial Haptics for Immersive Environments. In *Proceedings of the 2020 CHI Conference on Human Factors in Computing Systems* (Honolulu, HI, USA) *(CHI '20)*. Association for Computing Machinery, New York, NY, USA, 1–14. https://doi.org/10.1145/3313831.3376481